Published in final edited form as:
Atmos Environ. 2012 December ; 61: 253–264. doi:10.1016/j.atmosenv.2012.06.088.

Mobile monitoring of particle number concentration and other traffic-related air pollutants in a near-highway neighborhood over the course of a year

Luz T. Padró-Martínez[1], **Allison P. Patton**[1], **Jeffrey B. Trull**[1,†], **Wig Zamore**[2], **Doug Brugge**[3], and **John L. Durant**[1,*]

[1]Department of Civil & Environmental Engineering, Tufts University, Medford, MA, USA

[2]Somerville Transportation Equity Partnership, Somerville, MA, USA

[3]Department of Public Health and Community Medicine, Tufts University, Boston, MA, USA

Abstract

Accurate quantification of exposures to traffic-related air pollution in near-highway neighborhoods is challenging due to the high degree of spatial and temporal variation of pollutant levels. The objective of this study was to measure air pollutant levels in a near-highway urban area over a wide range of traffic and meteorological conditions using a mobile monitoring platform. The study was performed in a 2.3-km^2 area in Somerville, Massachusetts (USA), near Interstate I-93, a highway that carries 150,000 vehicles per day. The mobile platform was equipped with rapid-response instruments and was driven repeatedly along a 15.4-km route on 55 days between September 2009 and August 2010. Monitoring was performed in 4–6-hour shifts in the morning, afternoon and evening on both weekdays and weekends in winter, spring, summer and fall. Measurements were made of particle number concentration (PNC; 4–3,000 nm), particle size distribution, fine particle mass ($PM_{2.5}$), particle-bound polycyclic aromatic hydrocarbons (pPAH), black carbon (BC), carbon monoxide (CO), and nitrogen oxides (NO and NO_x). The highest pollutant concentrations were measured within 0–50 m of I-93 with distance-decay gradients varying depending on traffic and meteorology. The most pronounced variations were observed for PNC. Annual median PNC 0–50 m from I-93 was two-fold higher compared to the background area (>1 km from I-93). In general, PNC levels were highest in winter and lowest in summer and fall, higher on weekdays and Saturdays compared to Sundays, and higher during morning rush hour compared to later in the day. Similar spatial and temporal trends were observed for NO, CO and BC, but not for $PM_{2.5}$. Spatial variations in PNC distance-decay gradients were non-uniform largely due to contributions from local street traffic. Hour-to-hour, day-to-day and season-to-season variations in PNC were of the same magnitude as spatial variations. Datasets containing fine-scale temporal and spatial variation of air pollution levels near highways may help to inform exposure assessment efforts.

*corresponding author: 016 Anderson Hall, Tufts University, Medford, MA, USA; 001-617-627-5489; john.durant@tufts.edu.
†Current address: 22 Nash Street, New Haven, CT, USA

Keywords

traffic-related air pollution; highway; urban; temporal variation; spatial variation; mobile monitoring

1. Introduction

Proximity to major roadways and exposure to motor vehicle exhaust emissions are associated with increased risks of cardiovascular, respiratory and other diseases (Brugge et al., 2007; Gan et al., 2010; Gauderman et al., 2007; Jerrett et al., 2009; Laden et al., 2007; McConnell et al., 2006). Specific pollutants in vehicle exhaust, including black carbon, polycyclic aromatic hydrocarbons, volatile organic compounds, and particulate matter, have been implicated as possible disease-causing agents; however, accurate exposure assessment, an essential part of establishing causality, is challenging in the near-highway environment due to the high degree of spatial and temporal variation in pollutant levels. This is particularly true for ultrafine particles (UFP; aerodynamic diameter <100 nm), which can be highly elevated in number concentration near roadways depending on spatially- and temporally-variable factors. Because UFP are more toxic per unit mass than particles with larger diameters (Dockery and Stone, 2007; Oberdörster et al., 1995) and can be translocated throughout the body (Choi et al 2010; Kreyling et al., 2006), there is considerable interest in understanding their possible role in disease causation.

Previous studies have shown that concentrations of UFP (as well as other primary pollutants in vehicular emissions) are elevated near busy roadways but then decrease to background levels within several hundred meters due to dilution and reactions (Karner et al., 2010 and references therein). The factors that impact the magnitude and extent of distance-decay gradients include traffic conditions, wind speed and direction, topography, atmospheric stability, and mixing height (Hagler et al., 2009, 2010; Hitchins et al., 2000; Hu et al., 2009; Zhu et al. 2006). While these studies, and many others, have made important contributions to our understanding of the extent and causes of spatiotemporal pollutant dynamics near busy roadways, we do not have a complete understanding of the extent to which pollutant distance-decay gradients change over time (e.g., hours, days and seasons) and space in near-roadway neighborhoods.

The goal of this work was to characterize both the spatial and temporal variation of traffic-related air pollutants in an urban neighborhood near a highway. Our specific objectives were to collect a dataset that reflected the range of spatial and temporal scales of air pollutant variation in the neighborhood over the course of one year, and to determine the major trends in pollutant concentrations. This work was done as part of the Community Assessment of Freeway Exposure and Health (CAFEH) study, a community-based participatory research study of near-highway air pollution and cardiovascular health in Somerville and other communities in and around Boston, Massachusetts (USA). This paper focuses on data collected in Somerville between September 2009 and August 2010. To capture the spatial variation in pollutant levels in Somerville we used a mobile platform that contained rapid response instruments for measuring ultrafine particles as well as fine particle mass ($PM_{2.5}$), particle-bound polycyclic aromatic hydrocarbons, black carbon, carbon monoxide, nitric oxide and total nitrogen oxides. To capture temporal variation due to differences in meteorology and pollutant source strength, mobile monitoring was performed at different times of the day, on different days of the week, and in different seasons of the year.

2. Methods

2.1 Study Area

Mobile monitoring was performed in a 2.3-km^2 area near Interstate 93 (I-93) in the northeastern part of Somerville (Figure 1). I-93 is a 40-m-wide highway with four northbound and four south-bound lanes, and it has an average traffic volume of ~150,000 vehicles per day (vpd; CTPS, 2012). The 2.4-km-long highway section within our study area rises from grade to as high as 5 m above street level and is filled underneath except at underpasses (three in the study area). There is a 3-m-high concrete noise barrier that extends ~500 m on the east side of the north-bound lane. The presence of a noise barrier is of importance because these structures can impact pollutant concentrations near highways (Bowker et al., 2007). Two other major roadways run through the study area at grade: (i) Massachusetts Route 38, a four-lane highway that runs parallel to I-93 with >30,000 vpd; and (ii) Massachusetts Route 28, a six-lane highway that crosses underneath I-93 and carries ~50,000 vpd (CTPS, 2012). The study area is thickly settled (population density = 11,200 km^{-2}) and contains many single- two- and three-family houses as well as low-rise apartment buildings. Other than traffic (i.e., on I-93, Rte 28, Rte 38 and local streets) and residential heating, the only known significant sources of air pollution in or near the study area include a natural gas- and oil-fired power plant (Constellation Energy Mystic Station), the bus depot at Sullivan Station, and diesel trains on the commuter rail line (~46 per weekday; 12 per weekend day).. All of these non-traffic sources are located east of the study area (see Figure 1), and when the winds are out of the west, the predominant wind direction in the region, these sources are downwind of the study area.

2.2 Mobile Monitoring

Real-time measurements of air pollutants were made with the Tufts Air Pollution Monitoring Laboratory (TAPL), a mobile platform equipped with fast-response instruments for monitoring gas- and particle-phase pollutants. The TAPL is a converted recreational vehicle (2003 Chevrolet chassis with a Vortec 8.1 V8 gas engine (odometer = 73,000 mi)), which is powered by two, 1.6-kW generators that are exhausted at the rear of the vehicle. The TAPL was driven slowly (5–10 m/s) to allow measurement of local-scale (~20 m) changes in pollutant concentrations. Individual measurements were matched to location by 1-second-interval GPS readings. The monitoring route (Figure 1) was designed to characterize the area in which the health-study participants lived, and consisted of both a near-highway neighborhood <400 m from the highway on either side, and a background neighborhood >1000 m from the west side of I-93 (note: 28% of the study participants lived <100 m from the highway, 50% within 100–400 m and the remainder >1000 m). The circuit around the near-highway neighborhood took ~1 hr to complete and was driven 5 or 6 times on each day of monitoring. Monitoring of the background neighborhood was performed every other circuit of the near-highway neighborhood (i.e., 2 or 3 times per monitoring day). On days when particle size distribution monitoring was performed, the mobile lab was parked for five minutes at each fixed monitoring location to allow collection of two complete scans of the particle size range. The dates and times of mobile monitoring are shown in Table 1.

The monitoring equipment in the TAPL is listed in Table 2. Total particle number concentrations (PNC; 4–3,000 nm) were measured using a condensation particle counter (CPC; Model 3775, TSI). Particle size distributions (6–213 nm) were measured with a Scanning Mobility Particle Sizer (SMPS; Model 3080 electrostatic classifier and a Model 3085 Nano DMA, TSI). The up and down scan times were 120 s and 15 s, respectively; only the data collected during the up scan was used for analysis. The sheath-to-sample flow ratio was 6.67:1. Particle-bound polycyclic aromatic hydrocarbons (pPAH) were measured with a

photoelectric aerosol sensor (PAS, Model PAS2000, EcoChem Analytics, Inc.), black carbon (BC) was measured with an aethalometer (Model AE-16, Magee Scientific), and $PM_{2.5}$ (particles with aerodynamic diameter ≤2.5 μm) was measured with a laser photometer (Sidepak AM510, TSI). Nitric oxide (NO) and nitrogen oxides (NO_x; sum of NO_2 and NO concentrations) were measured using a chemiluminescence analyzer (Model 42i, Thermo Scientific). Carbon monoxide (CO) was measured using a gas filter correlation analyzer (Model 48i-TLE, Thermo Scientific). The measurement frequency of each instrument is listed in Table 2. No measurements for pPAHs, $PM_{2.5}$, and BC were recorded before 20 September 2009, 20 February 2010 and 9 June 2010, respectively.

Wind speed, wind direction, air temperature and relative humidity were recorded every five minutes at the Hormel Stadium light tower (height ~35 m; wunderground.com), which is ~1.6 km north from the study area (Figure 1). Prior to analysis, wind speed was standardized to 3 m above ground level (i.e., the height of the inlet on the TAPL) assuming a power law wind profile with p=0.55. When meteorological data from the Hormel station were not available, data from the Mystic Activity Center (MAC) station were used (Figure 1) (Hemphill Fuller et al., 2012). Hourly vehicle counts for I-93 (station #8449; located near the southeast corner of Ten Hills on I-93) were provided by the Massachusetts Department of Transportation Highway Division (stakeholder.traffic.com).

2.3 Data Quality Assurance

2.3.1 Particle Measurements—The particle inlet manifold was made of stainless steel. All tubing on instrument inlets was either Tygon or conductive-silicon tubing; conductive-silicon tubing was also used to connect the DMA to the CPC to minimize particle loss due to electrostatic deposition. Tubing to the PAS and aethalometer was made of aluminum. The length of the tubing from the manifold to each instrument was minimized to reduce particle loss due to sorption. The CPC was manufacturer-calibrated just prior to the start of the monitoring campaign in September 2009. Side-by-side comparison of the mobile laboratory CPC with an identical unit at the end of the study period resulted in an R^2 of 0.96 with paired measurements differing by <3%. The two CPCs had <10% difference in their measurements for 96.2% of all measurements and <20% difference for 99.7% of all measurements, which was within the instrument specifications. At the start of each monitoring session, the instrument-reported flow rate through the CPC was checked (Defender 510-H, Bios International), and a polyethersulfone membrane filter (rated at 99.96% removal efficiency for 0.45 μm particles) was placed on the inlet to check that the PNC dropped to <100 particles per cm^3. During monitoring, the CPC was watched for flow rate errors, which were usually caused by butanol in the air lines (flooding). The frequency of flooding was minimized by turning off the autofill setting on the CPC when the TAPL drove on steep hills or >65 kmph (18 m/s) on the highway. When flow rate errors occurred, the instrument was opened and checked for flooding. If butanol was found in the gas lines, they were drained and the CPC was run dry for 24 h to remove residual butanol.

The Sidepak was calibrated by the manufacturer at the start of the monitoring campaign and again in February 2010. Prior to each day of monitoring, a zero calibration was performed with a polyethersulfone membrane filter (same as that used for the CPC zero check). The PAS was also manufacturer-calibrated prior to the start of the monitoring campaign. The external pump on the aethalometer was checked monthly and adjusted as necessary to the no-load pump flow rate of 5.5 Lpm.

2.3.2 Gas Measurements—The gas inlet manifold was made from Teflon tubing and contained a 0.45-μm Teflon filter. The calibrations of the gas instruments were checked prior to each monitoring session. The CO and NO_x monitors were allowed to warm up for at

least 90 min prior to calibration. In cold temperatures (<10 °C), the warm-up time was extended to ≥2 hours to ensure stable readings. After the instruments had warmed up, the calibrations were checked with 0 ppm and 1 ppm NO (Airgas) and 0 ppm and 4 ppm CO (Airgas). If the validation showed deviations in excess of ±0.003 ppm NO or ±0.03 ppm CO, a single point calibration of the appropriate monitor was conducted. A calibrator (Model 146, TSI) controlled the flow of calibration gases and generated zero NO gas; the CO monitor internally generated zero CO gas. Halfway through each monitoring session, the zero CO concentration was checked against zero CO gas and the instrument automatically adjusted itself as necessary.

2.4 Data Processing and Analysis

Data from all of the instruments was aggregated in MySQL (www.mysql.com) using PHP scripts; post-processing for quality control was performed using Excel VBA macros and by inspection of time-series plots. Data processing consisted of several steps. First, measurements associated with instrument errors, as noted in the daily log, were removed. When CPC flooding was suspected but could not be confirmed by direct observation, confirmation was performed by comparison of TAPL data with CPC measurements made at the MAC site (Figure 1) (Hemphill Fuller et al., 2012). Next, the timestamps for measurements from each instrument were corrected for the time lag between entry of air into the inlet and the time when concentrations are recorded by the instrument. Lag times were measured as the time for particles and gases introduced at the inlet (i.e., as smoke from a lit match) to be sensed by the instrument (Table 2). The final step was to remove data that reflected self-monitoring of exhaust from the TAPL. Self-monitoring was possible when the TAPL was stopped at traffic lights or in slow-moving traffic, especially if the wind was from behind. Self-monitoring was minimized by locating the gas and particle inlets on the roof of the vehicle near the front of the TAPL, ~5 m horizontally and 2 m vertically from the exhaust tailpipe. Based on experiments conducted at Tufts prior to the start of the monitoring campaign (results not shown), data was excluded when the following three conditions were simultaneously met: (1) the TAPL speed was <5 kmph (1.4 m/s), (2) the wind was coming from behind the TAPL, and (3) the wind speed was greater than the speed of the TAPL. Overall, 14% of the data from each monitoring day was removed due to self-monitoring; the majority (>90%) of the removed data was collected when the TAPL was stopped at traffic lights. Pollutant spikes due to other vehicles nearby the TAPL, as confirmed by the written daily log, were not removed from the dataset unless the data exclusion rules were violated.

Pollutant concentration maps were generated in ArcGIS 9.3.1 using version-2008 data layers downloaded from MassGIS (2010). To facilitate data interpretation, the mobile monitoring data was divided into bins of varying width oriented parallel to I-93. The study area southwest of I-93 was divided into 7 bins (0–50, 50–100, 100–150, 150–200, 200–350, 350–650, and 1000–1800 m as measured from the southwest edge of I-93), while the study area northeast of I-93 was divided into 5 bins (0–50, 50–100, 100–150, 150–200, and 200–450 m as measured from the northeast edge of I-93). Box plots of binned data as well as scatter plots of the unbinned data were made using IGOR Pro (Version 5; WaveMetrics, Inc.).

3. Results and Discussion

3.1 Monitoring conditions

Monitoring was performed on a total of 58 different days between September 10, 2009 and August 26, 2010 including 55 mobile-monitoring days (5–6 h each day) and three stationary-monitoring days (during which the TAPL was parked at a single location for 24 hr) (Table 1). Mobile monitoring was performed on 18 winter days, 13 spring days, 12

summer days, and 12 fall days. The majority of monitoring was done on weekday mornings (n=29 sessions) to allow characterization of worst-case conditions in terms of traffic volume (rush hour) and atmospheric mixing (the atmosphere is relatively stable near land surfaces in the morning). The least amount of monitoring was done on weekend days after 10:30 (n=4 sessions). Overall, 32% of the mobile monitoring measurements were made within 100 m of I-93, 34% between 100–400 m, 17% between 400–1,000 m and 17% between 1,000–1,800 m of the highway. Traffic data Figure 2 (top panel) show that for each hour of monitoring the traffic volume on I-93 was generally representative of the annual average for that hour. The data in Figure 3 indicate that during monitoring the winds were mostly from the west and west-northwest at between 2 and 8 m/s, reflecting annual patterns. Hourly average wind speed and direction for the years immediately preceding and following the study period were not significantly different compared to the study period ($p<0.05$ based on a Student's t-test). Monitoring was performed during only four precipitation events. This number is low – there were 147 days of precipitation during the entire study period – in part because monitoring was not performed when the driving conditions were likely to be unsafe (i.e., when there was snow on the roads, during heavy rain storms or when lightning was forecast).

3.2 Correlations

A scatter plot matrix of 120-s-averaged pollutant concentrations measured between 05:20 and 10:50 on June 9, 2010 is shown in Figure S1. The measurements were made during five circuits of the near-highway monitoring route including three of the background area. The non-parametric Spearman correlation ρ^2 was used to test for statistical significance because the pollutant frequency distributions were consistent with being log-normal. The results in Table 3 show that PNC was correlated with NO, NO_x and pPAH, NO was correlated with pPAH, and NO_x was correlated with CO, NO and NO_2 ($\rho^2 > 0.7$); the other pollutants had lower correlation values ($\rho^2 < 0.7$). Westerdahl et al. (2005) reported ρ^2 values as high as 0.9 for markers of diesel emissions (e.g., PNC vs. NO, PNC vs. pPAH, BC vs. pPAH) on busy roadways in Los Angeles. Our lower values here likely reflect both the smaller fraction of diesel vehicles traveling on I-93 (1–5%) compared to the highways driven in LA (1.3–14%), and the relatively greater degree of mixing and pollutant transformation within our *near-highway* neighborhood as compared to the *on-highway* route (with fresher emissions) studied by Westerdahl et al. (2005). When we performed the same analysis with data collected in the Central Artery Tunnel, a 2.4-km tunnel running through downtown Boston, we obtained ρ^2 values (data not presented here) generally higher than those in Table 3, but not as high as those reported by Westerdahl et al. (2005).

3.3 Spatial and temporal variation of PNC

As illustrated in Figure 4, PN concentrations were highest near I-93 with distance-decay gradients extending up to 100–150 m on the southwest side of the highway and >200 m on the northeast side. A plot of all the data from all the monitoring sessions (Figure 4a) shows that the median PNC in the 0–50 m bin (3.7×10^4 cm^{-3}) was 1.5-times higher than in both the 200–450 m bin on the northeast side of I-93 and the 100–150 m bin on the southwest side, and 2.1-times higher than in the 1000–1800 m bin on the southwest side of the highway. The area in this latter bin is characterized by residential streets with relatively little traffic, and is thus considered indicative of urban background pollution levels. In contrast, the area represented by the four bins between 100 and 650 m on the southwest side of I-93 contains more heavily trafficked streets, which likely accounts for the higher PN concentrations.

Figures 4b–4d illustrate the variation in PNC distance-decay gradients as a function of season, day of the week and time of day. PN concentrations were consistently highest in all data bins during the winter, next highest during the spring, and lowest during the summer

and fall (Figure 4b). These trends are attributable to generally higher PNC levels in vehicle exhaust emissions and greater atmospheric stability (less vertical mixing) during colder months (Charron and Harrison, 2003; Hinds, 1999; Jacob, 1999), and are consistent with seasonal PNC measurements reported elsewhere (e.g., Hussein et al., 2007; Wang et al., 2011). As shown in Figure 4c, PNC levels were higher on the northeast side of I-93 on weekdays compared to Saturdays and higher on the southwest side on weekends compared to weekdays. This difference likely reflects wind patterns (winds were out of the west ~73% of the monitoring time) and differences in local street traffic on the two sides of the highway (more commercial traffic on the southwest side). The consistently low PN concentrations on Sundays are attributable in part to the study design: relatively few Sunday monitoring sessions were conducted (n=4) and of these only two were conducted after 10:30 when Sunday traffic volume on I-93 was highest (Figure 2). PNC distance-decay gradients as a function of time of day are shown in Figure 4d. On the northeast side of I-93, PN concentrations were consistently highest during the morning (05:00–09:00) followed by midday (09:00–15:00). Also, despite relatively high levels of highway traffic, PN concentrations on the northeast side of I-93 were lower in the late afternoon (15:00–21:00) likely due to increasing winds, and hence mixing, toward sunset. In contrast, afternoon PN concentrations on the southwest side were higher than at midday and, in some bins, higher than in the morning, likely reflecting local traffic contributions to PNC in the late afternoon. This is consistent with the findings of Hu et al. (2012) who reported that high-emitting vehicles on local streets contributed to elevated PNC throughout the day in a Los Angeles neighborhood near several highways. A comparison of median PN concentrations in Figure 4 indicates that maximum hour-to-hour, day-to-day and season-to-season variations in PNC were of the same magnitude as the maximum spatial contrast in PNC. These results differ from those of Bukowiecki et al. (2003) who found that temporal variation exceeded spatial variation of PNC in a year-long study conducted in and around Zürich (CH).

The box plots in Figure 5 show the relationship between wind direction and wind speed and PNC-distance-decay gradients near I-93. As expected, for winds out of the southwest and northwest, PN concentrations were elevated on the northeast side of I-93 relative to the southwest side, and when winds were out of the northeast the opposite occurred. These observations indicate that when winds are out of the northeast, southwest and northwest, I-93 is the dominant source of PNC to receptor areas immediately downwind of the highway. Interestingly, the highest PN concentrations in all bins were measured when the winds were out of the southeast (Figure 5a), possibly reflecting contributions from sources to the southeast of the study area. However, southeast winds occurred infrequently (11.6% of the time during the entire year; 7.9% of the monitoring time), which is why in the composite figure (4a) PN concentrations on the southwest side of I-93 are much lower relative to the northeast side. As shown in Figure 5b, PNC was also greatly impacted by wind speed: median PN concentrations in all bins were highest for calm winds (<0.3 m/s) and lowest for wind speeds >1.6 m/s. Winds from the southeast were typically calm, which further explains the high PN concentrations in the study area when winds were from this sector.

It should be noted that the x-axis in Figures 4 and 5 was measured with respect to the edges of I-93 as defined in the MassGIS highways and major roadways data layer. Measurements made in the Shore Drive, Temple Street, and Fellsway (Rte 28) underpasses were excluded from the graphs (PN concentrations in these underpasses were comparable to concentrations measured in the 0–50 m bins). It should also be noted that on-highway PN concentrations (measured in a separate study) were comparable to off-highway levels: based on 33 southbound and 34 northbound traverses of I-93 through the study area between 13 September 2010 and 28 June 2011, the median on-highway PNC (3.7×10^4 cm^{-3}) was no

different than in the 0–50 m bins, suggesting a high degree of mixing in the immediate vicinity of the highway.

The plots in Figure 6 show the spatial distribution of PNC over the entire study area based on several hours of monitoring on a winter day (January 6, 2010). Each plot represents one circuit of the mobile lab through the study area or ~1 h of PNC measurements collected at a frequency of 1 s^{-1}. The plots show that PNC throughout the study area were generally highest in the early morning (06:00–08:00). The late morning decrease is likely due to increasing dilution attributable to higher wind speeds and the lifting of the surface boundary layer after sunrise. These results are consistent with mobile monitoring measurements made in the same area on a comparable January day in 2008 (Durant et al., 2010). In this previous study PNC on the northeast (downwind) side of I-93 exhibited sharply-defined distance-decay gradients before 08:00 and much less pronounced gradients after 09:00. We observed similar temporal variation in the distance-decay gradients in the 2010 dataset. Taken together, these two studies demonstrate the effects of post-sunrise mixing in reducing near-highway PN concentrations.

3.4 Particle size-distribution measurements

Particle size distribution monitoring was performed on 11 days during the winter and spring. Emphasis was placed on characterizing short-term (i.e., a few hours) changes in size distribution as a function of distance from I-93. Monitoring was performed by parking the mobile lab for ~5 minutes (enough time for two full 135-s scans of the particle size range) at each of several fixed sites along Temple Street (southwest side) and Temple Road (northeast side), a continuous roadway that is roughly orthogonal to I-93. Our results are summarized in Figure 7, which compares the pre-sunrise (maximum atmospheric stability) and post-sunrise particle size distribution along Temple Road on four mornings. The results indicate there were no significant differences in particle size distributions either with distance from I-93 or over time. Particles 6–50 nm in aerodynamic diameter (nuclei mode) dominated the particle size distribution measurements both pre-sunrise and post-sunrise on all four days; nearly 80% of particles in the 6–213 nm size range were <50 nm. Also, the relative number concentrations of 50–213 nm particles did not substantially change with distance from I-93, a finding that is consistent with previous research in the study area (Durant et al., 2010) as well as with other near-highway studies (Hu et al, 2009; Zhu et al., 2006).

3.5 Spatial and temporal variation of other air pollutants

Spatial variation of NO_x for all monitoring times as a function of time of day, day of the week and season are shown in Figure 8; spatial variation of NO, CO, pPAH, $PM_{2.5}$ and BC for all monitoring times are shown in Figure 9. Figures similar to Figure 8 for NO, CO, pPAH, $PM_{2.5}$ and BC appear as Supplemental Figures (S2–S6). These figures indicate that the spatial and temporal trends of NO_x, NO, CO, pPAH and BC were consistent with PNC while those of $PM_{2.5}$ were not. As show in Figure 8, the highest NO_x concentrations were measured in the 0–50 m bins on either side of I-93 and the concentrations decayed to background levels within ~200 m. Likewise, NO_x levels were highest in winter and lowest in summer and fall, higher on weekdays compared to weekends, and higher during the morning rush hour as compared to later in the day. Also, as was observed for PNC in Figure 5, relatively high levels of NO_x were observed for calm winds (<0.3 m/s) and for winds out of the southeast (results not shown). Similar distance-decay gradients were observed for NO, CO, pPAH, and BC (Figure 9(a–d)). The increased levels of NO and CO in the 200–350-m and 350–650-m bins on the southwest side of I-93 relative to bins closer to the highway likely reflects the influence of fresh emissions from local street traffic. In contrast, the distance-decay gradients for $PM_{2.5}$ (Figure 9(e)) were relatively flat, consistent with $PM_{2.5}$ deriving from regional sources. These results suggest that with the exception of $PM_{2.5}$ the

other pollutants are elevated in concentration near I-93 and they are influenced by the same meteorological forcings that impact the distribution of PNC near the highway. $PM_{2.5}$ levels were also elevated during spring and summer relative to winter, consistent with secondary aerosol growth (Figure S6).

3.6 Significance

The data we collected during the mobile monitoring campaign allow us to characterize traffic-related air pollution in the study area and provide insight into the main factors that affect the spatial and temporal variation of pollutant levels. Our results are consistent with the findings of previous studies that have used mobile monitoring to characterize the near-roadway environment (Bukowiecki et al., 2003; Hu et al., 2012; Jiang et al., 2005; Larson et al., 2009; Pirjola et al., 2006; Westerdahl et al., 2005; Zwack et al., 2011). These studies highlight the importance of collecting finely-resolved spatial and temporal data for a broad suite of pollutants and environmental factors. Our study adds to this body of knowledge by demonstrating the utility of a year-long mobile monitoring campaign for characterizing daily, weekly and seasonal variations in the spatial distribution of traffic-related air pollutants within ~1 km of an urban highway.

One limitation of our study has to with self-sampling. To avoid inclusion of self-sampling in our dataset, we removed 14% of the measurements. Of these, the majority represented times when the TAPL was stopped at traffic lights and stop signs in commercial areas. Our decision rules for removing self-sampling and the amount of data we removed are consistent with previous studies involving fossil-fuel-powered mobile monitoring platforms. For example, Bukowiecki et al. (2002) reported <5% self-sampling while monitoring with a diesel-powered mobile lab in urban, suburban and rural areas around Zürich, and Jiang et al. (2005) reported 40% self-sampling while monitoring with a gasoline-powered lab in Mexico City. Looking more closely at our data, when we recreated Figures 4 and 5 without removing any of the self-sampling measurements, there was no significant difference in median PNC values or the inter-quartile ratios. This indicates that removal of self-sampling did not bias our results, and therefore, does not impact our overall conclusions.

Another limitation of our approach was the potential bias in the monitoring schedule. Specifically, it was challenging to develop a representative characterization of air pollution given the range and possible combinations of traffic and meteorological conditions for our monitoring area and the period of our study. For example, air pollution levels during wet weather are underrepresented in our dataset. A solution to this is to use a hybrid approach in which data from a stationary site(s) – preferably one within or as near to the study area as possible is used to inform critical temporal gaps in the mobile monitoring dataset.

3.7 Conclusions

This study demonstrates the utility of a mobile monitoring platform for characterizing fine-scale spatial and temporal variations of traffic-related air pollution in a near-highway urban neighborhood. By monitoring on 55 days throughout a 1-y period we were able to measure hour-to-hour, day-to-day, and season-to-season variation in air pollution levels. We observed substantial variation in the levels of fresh combustion emissions - PNC, NO, pPAH, and CO, with the extent of variation depending on time of day and meteorological conditions. In general, traffic-related air pollutant levels were highest in the morning compared to later in the day, higher on weekdays and Saturdays than Sundays, and highest in winter compared to the other three seasons. While the highway was a substantial contributor of pollution to the neighborhood, it is clear that high-emitting vehicle traffic on local streets is also an important source of pollutants. This dataset could be useful for developing a predictive air pollution model for use in exposure assessment.

Supplementary Material

Refer to Web version on PubMed Central for supplementary material.

Acknowledgments

We are grateful to Eric Wilburn, Piers MacNaughton, Kevin Stone, Tim McAuley, Samantha Weaver and Jessica Perkins for help with the data collection and processing effort. The CAFEH Steering Committee including Ellin Reisner, Baolian Kuang, Michelle Liang, Christina Hemphill Fuller, Lydia Lowe, Edna Carrasco, M Barton Laws and Mario Davila provided invaluable assistance in planning the data collection effort. We are also grateful to George Allen at NESCAUM for the generous loan of the aethalometer. This research was funded by the National Institute of Environmental Health Sciences (Grant No. ES015462) and the Tisch College (through the Tufts Community Research Center). AP also received funding from a US EPA STAR Fellowship Assistance Agreement (No. FP-91720301-0) and JT received support from the Department of Civil & Environmental Engineering at Tufts.

References

Bowker GE, Baldauf R, Isakov V, Khlystov A, Petersen W. The effects of roadside structures on the transport and dispersion of ultrafine particles from highways. Atmospheric Environment. 2007; 41:8128–8139.

Brugge D, Durant JL, Rioux C. Near-highway pollutants in motor vehicle exhaust: A review of epidemiologic evidence of cardiac and pulmonary health risks. Environmental Health. 2007; 610.1186/1476-069X-6-23

Bukowiecki N, Dommen J, Prevot ASH, Richter R, Weingartner E, Baltensperger U. A mobile pollutant measurement laboratory—measuring gas phase and aerosol ambient concentrations with high spatial and temporal resolution. Atmospheric Environment. 2002; 36:5569–5579.

Bukowiecki N, Dommen J, Prevot ASH, Weingartner E, Baltensperger U. Fine and ultrafine particles in the Zurich (Switzerland) area measured with a mobile laboratory: An assessment of the seasonal and regional variation throughout a year. Atmospheric Chemistry and Physics. 2003; 3:1477–1494.

Central Transportation Planning Staff (CTPS) Geoserver. [Accessed June 5, 2012] Average Daily Traffic on Massachusetts Roads. 2012. http://www.ctps.org/geoserver/www/apps/adtApp/index.html

Charron A, Harrison RM. Primary particle formation from vehicle emissions during exhaust dilution in the roadside atmosphere. Atmospheric Environment. 2003; 37:4109–4119.

Choi HS, Ashitate Y, Lee JH, Kim SH, Matsui A, Insin N, Bawendi MG, Semmler-Behnke M, Frangioni JV, Tsuda A. Rapid translocation of nanoparticles from the lung airspaces to the body. Nature Biotechnology. 2010; 28:1300–1303.

Dockery DW, Stone PH. Cardiovascular risks from fine particulate air pollution. New England Journal of Medicine. 2007; 356:511–513. [PubMed: 17267912]

Durant JL, Ash CA, Wood EC, Herndon SC, Jayne JT, Knighton WB, Canagaratna MR, Trull JB, Brugge D, Zamore W, Kolb CE. Short-term variation in near-highway air pollutant gradients on a winter morning. Atmospheric Chemistry and Physics. 2010; 10:8341–8352.

Gan WQ, Tamburic L, Davies HW, Demers PA, Koehoorn M, Brauer M. Changes in residential proximity to road traffic and the risk of death from coronary heart disease. Epidemiology. 2010; 21:642–649. [PubMed: 20585255]

Gauderman WJ, Vora H, McConnell R, Berhane K, Gilliland F, Thomas D, Lurmann F, Avol E, Kunzli N, Jerrett M, Peters J. Effect of exposure to traffic on lung development from 10 to 18 years of age: A cohort study. Lancet. 2007; 369:571–577. [PubMed: 17307103]

Hagler GSW, Baldauf RW, Thoma ED, Long TR, Snow RF, Kinsey JS, Oudejans L, Gullet BK. Ultrafine particles near a major roadway in Raleigh, North Carolina: Downwind attenuation and correlation with traffic-related pollutants. Atmospheric Environment. 2009; 43:1229–1234.

Hagler GSW, Thoma ED, Baldauf RW. High-resolution mobile monitoring of carbon monoxide and ultrafine particle concentrations in a near-road environment. Journal of the Air & Waste Management Association. 2010; 60:328–336. [PubMed: 20397562]

Hemphill Fuller C, Brugge D, Williams PL, Mittleman MA, Durant JL, Spengler JD. Estimation of ultrafine particle concentrations at near-highway residences using data from local and central monitors. Atmospheric Environment. 2012; 57:257–265.

Hinds, WC. Aerosol technology: Properties, behavior and measurement of airborne particles. 2. John Wiley & Sons Inc; New York, New York: 1999.

Hitchins J, Morawska L, Wolff R, Gilbert D. Concentrations of submicrometre particles from vehicle emissions near a major road. Atmospheric Environment. 2000; 34:51–59.

Hu SS, Paulson SE, Fruin S, Kozawa K, Mara S, Winer AM. Observation of elevated air pollutant concentrations in a residential neighborhood of Los Angeles California using a mobile platform. Atmospheric Environment. 2012; 51:311–319.

Hu SS, Fruin S, Kozawa K, Mara S, Paulson SE, Winer AM. A wide area of air pollutant impact downwind of a freeway during pre-sunrise hours. Atmospheric Environment. 2009; 43:2541–2549.

Hussein T, Kukkonen J, Korhonen H, Pohjola M, Pirjola L, Wraith D, Härkönen J, Teinilä K, Koponen IK, Karppinen A, Hillamo R, Kulmala M. Evaluation and modeling of the size fractionated aerosol particle number concentration measurements nearby a major road in Helsinki Part II: Aerosol measurements within the SAPPHIRE project. Atmospheric Chemistry and Physics. 2007; 7:4081–4094.

Jacob, DJ. Introduction to Atmospheric Chemistry. Princeton University Press; Princeton, New Jersey: 1999.

Jerrett M, Finkelstein MM, Brook JR, Arain MA, Kanaroglou P, Stieb DM, Gilbert NL, Verma D, Finkelstein N, Chapman KR, Sears MR. A cohort study of traffic-related air pollution and mortality in Toronto, Ontario, Canada. Environmental Health Perspectives. 2009; 117:772–777. [PubMed: 19479020]

Jiang M, Marr LC, Dunlea EJ, Herndon SC, Jayne JT, Kolb CE, Knighton WB, Rogers TM, Zavala M, Molina LT, Molina MJ. Vehicle fleet emissions of black carbon, polycyclic aromatic hydrocarbons, and other pollutants measured by a mobile laboratory in Mexico City. Atmospheric Chemistry and Physics. 2005; 5:3377–3387.

Karner AA, Eisinger DS, Niemeier DA. Near-Roadway Air Quality: Synthesizing the Findings from Real-World Data. Environmental Science & Technology. 2010; 44:5334–5344. [PubMed: 20560612]

Kreyling WG, Semmler-Behnke MVD, Möller W. Ultrafine particle lung interactions: Does size matter? Journal of Aerosol Medicine. 2006; 19:74–83. [PubMed: 16551218]

Laden F, Hart JE, Smith TJ, Davis ME, Garshick E. Cause-specific mortality in the unionized US trucking industry. Environmental Health Perspectives. 2007; 115:1192–1196. [PubMed: 17687446]

Larson T, Henderson SB, Brauer M. Mobile monitoring of particle light absorption coefficient in an urban area as a basis for land use regression. Environmental Science & Technology. 2009; 43:4672–4678. [PubMed: 19673250]

MassGIS. Data layers retrieved from Office of Geographic Information (MassGIS). Commonwealth of Massachusetts, Information Technology Division; (http://www.mass.gov/mgis/massgis.htm)

McConnell R, Berhane K, Yao L, Jerrett M, Lurmann F, Gilliland F, Kunzli N, Gauderman J, Avol E, Thomas D, Peters J. Traffic, susceptibility, and childhood asthma. Environmental Health Perspectives. 2006; 114:766–772. [PubMed: 16675435]

NAVTEQ Traffic. [Accessed October 28, 2010] 2009. http://stakeholder.traffic.com/mainmenu/stakeholder.html

Oberdörster G, Gelein RM, Ferin J, Weiss B. Association of particulate air-pollution and acute mortality Involvement of ultrafine particles. Inhalation Toxicology. 1995; 7:111–124. [PubMed: 11541043]

Pirjola L, Paasonen P, Pfeiffer D, Hussein T, Hameri K, Koskentalo T, Virtanen A, Ronkko T, Keskinen J, Pakkanen TA, Hillamo RE. Dispersion of particles and trace gases nearby a city highway: Mobile laboratory measurements in Finland. Atmospheric Environment. 2006; 40:867–879.

Wang YG, Hopke PK, Chalupa DC, Utell MJ. Long-term study of urban ultrafine particles and other pollutants. Atmospheric Environment. 2011; 45:7672–7680.

Weather Underground. [Accessed November 6, 2010] http://www.wunderground.com/weatherstation/WXDailyHistory.asp?ID=KMAMEDFO7

Westerdahl D, Fruin S, Sax T, Fine PM, Sioutas C. Mobile platform measurements of ultrafine particles and associated pollutant concentrations on freeways and residential streets in Los Angeles. Atmospheric Environment. 2005; 39:3597–3610.

Zhu YF, Kuhn T, Mayo P, Hinds WC. Comparison of daytime and nighttime concentration profiles and size distributions of ultrafine particles near a major highway. Environmental Science & Technology. 2006; 40:2531–2536. [PubMed: 16683588]

Zwack LM, Hanna SR, Spengler JD, Levy JI. Using advanced dispersion models and mobile monitoring to characterize spatial patterns of ultrafine particles in an urban area. Atmospheric Environment. 2011; 45:4822–4829.

Highlights

- mobile monitoring was performed on 55 days throughout one year
- hourly, daily, and seasonal variations were observed
- distance-decay gradients were highly dependent on traffic and meteorology
- annual median PNC 0–50 m from the highway was two-fold higher than background
- temporal variations in PNC were similar to spatial variations

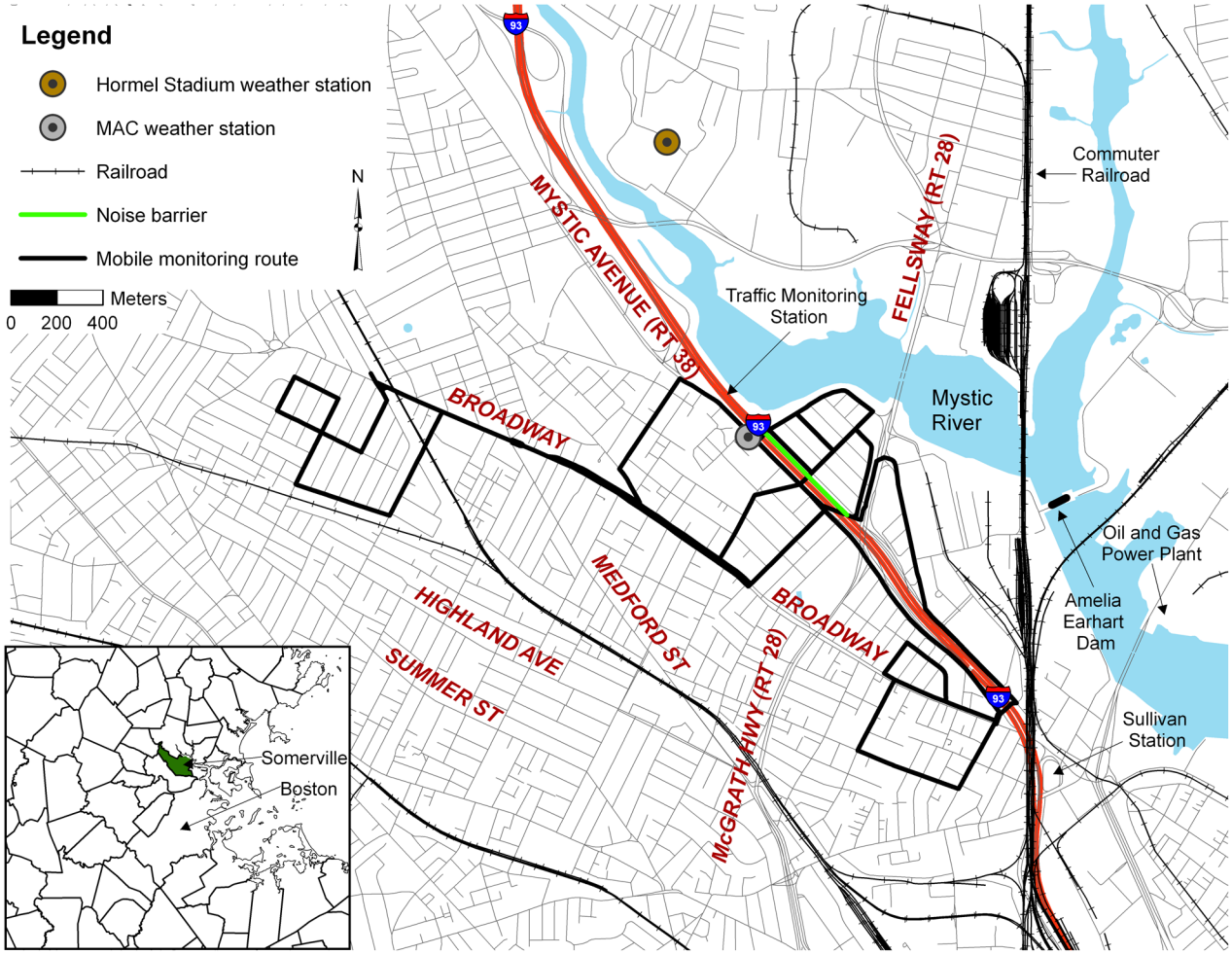

Figure 1.

Map of mobile-monitoring area in east Somerville. Traffic volumes on the monitoring route streets were as follows: Mystic Ave. ~30,000 vpd; Broadway Ave. between Medford St. and Rt. 28 ~8,000 vpd and east of Rt. 28 ~14,000 vpd; Rt. 28 south of I-93 ~ 39,000 vpd and north of I-93 ~60,000 vpd; all local roads <3,000 vpd (CTPS, 2012). Note: the railroad spurs on the west side of the commuter line just south of the Mystic River are no longer in use.

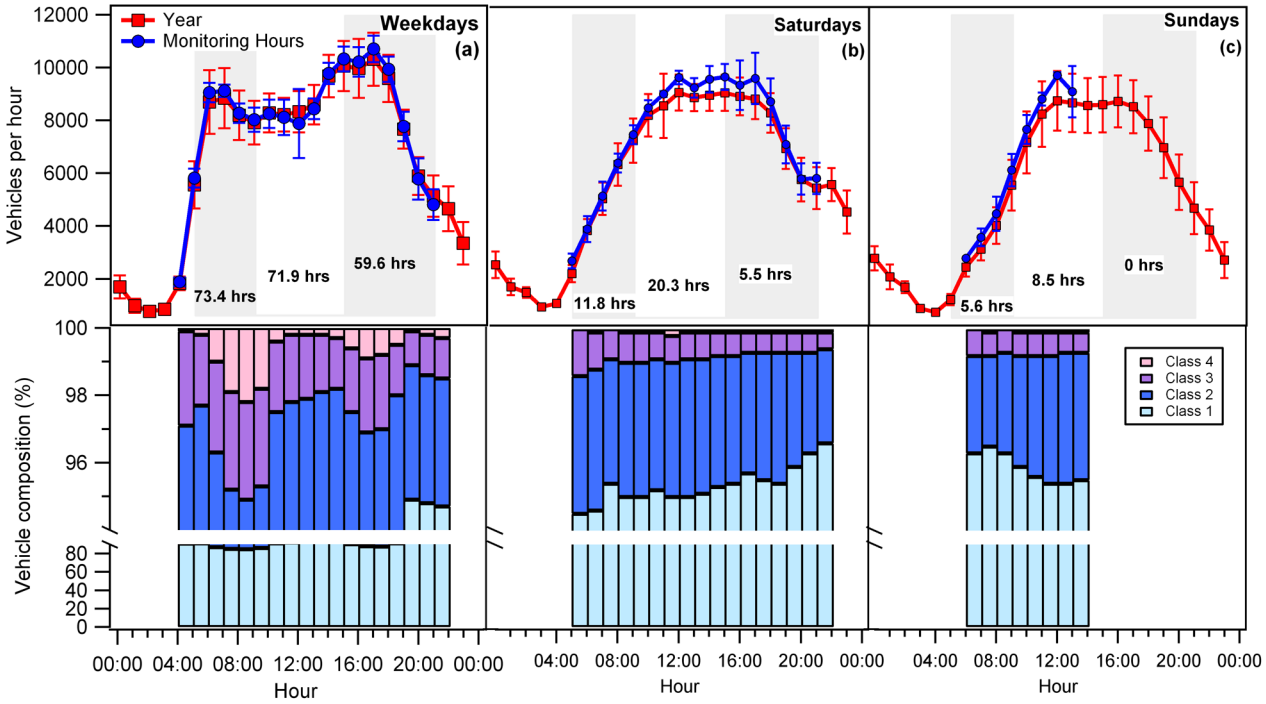

Figure 2.

(top panel) Time-series of traffic volume on I-93 (total of all lanes) for (a) weekdays, (b) Saturdays and (c) Sundays between September 10, 2009 and August 26, 2010. Year-long hourly averages (± one SD) are shown in red; hourly averages (± one SD) for each hour of monitoring are shown in blue. Total monitoring hours are shown for morning, midday, and afternoon monitoring periods for each type of day. (bottom panel) Annual average fleet composition per monitoring hour. Class 1 = motorcycles and passenger cars (FHWA classes 1–4); Class 2 = single-unit trucks and buses (FHWA classes 5–7); Class 3 = tractor trailers (FHWA classes 8–10); and Class 4 = multiple trailers (FHWA classes 11–13). Class 3 and 4 and an unknown fraction of class 2 vehicles run on diesel fuel.

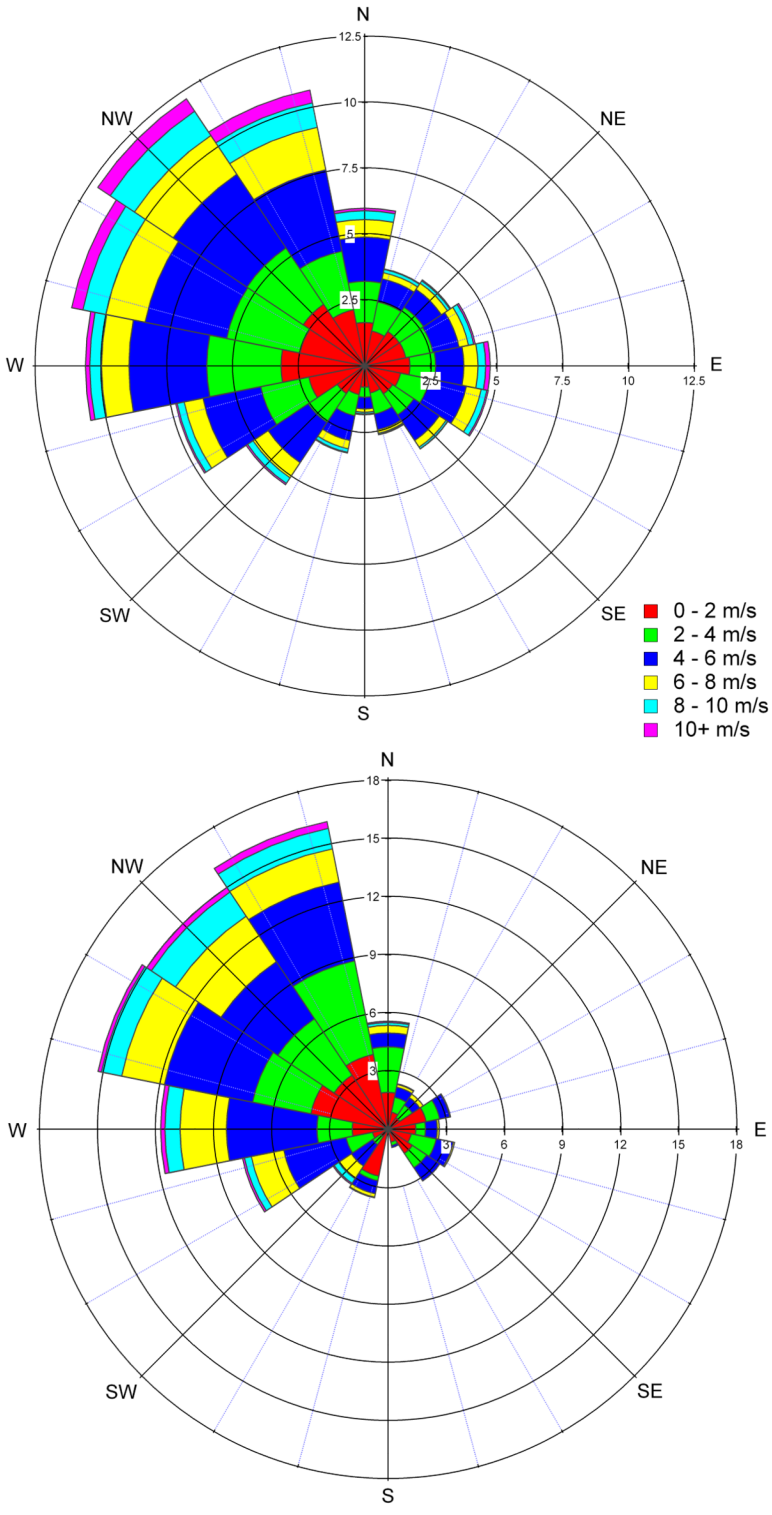

Figure 3.

5-min average wind speed and direction for (a) all times and (b) when mobile monitoring was performed between September 10, 2009 and August 26, 2010. These measurements were made at the Hormel Stadium station at an elevation of 35 m.

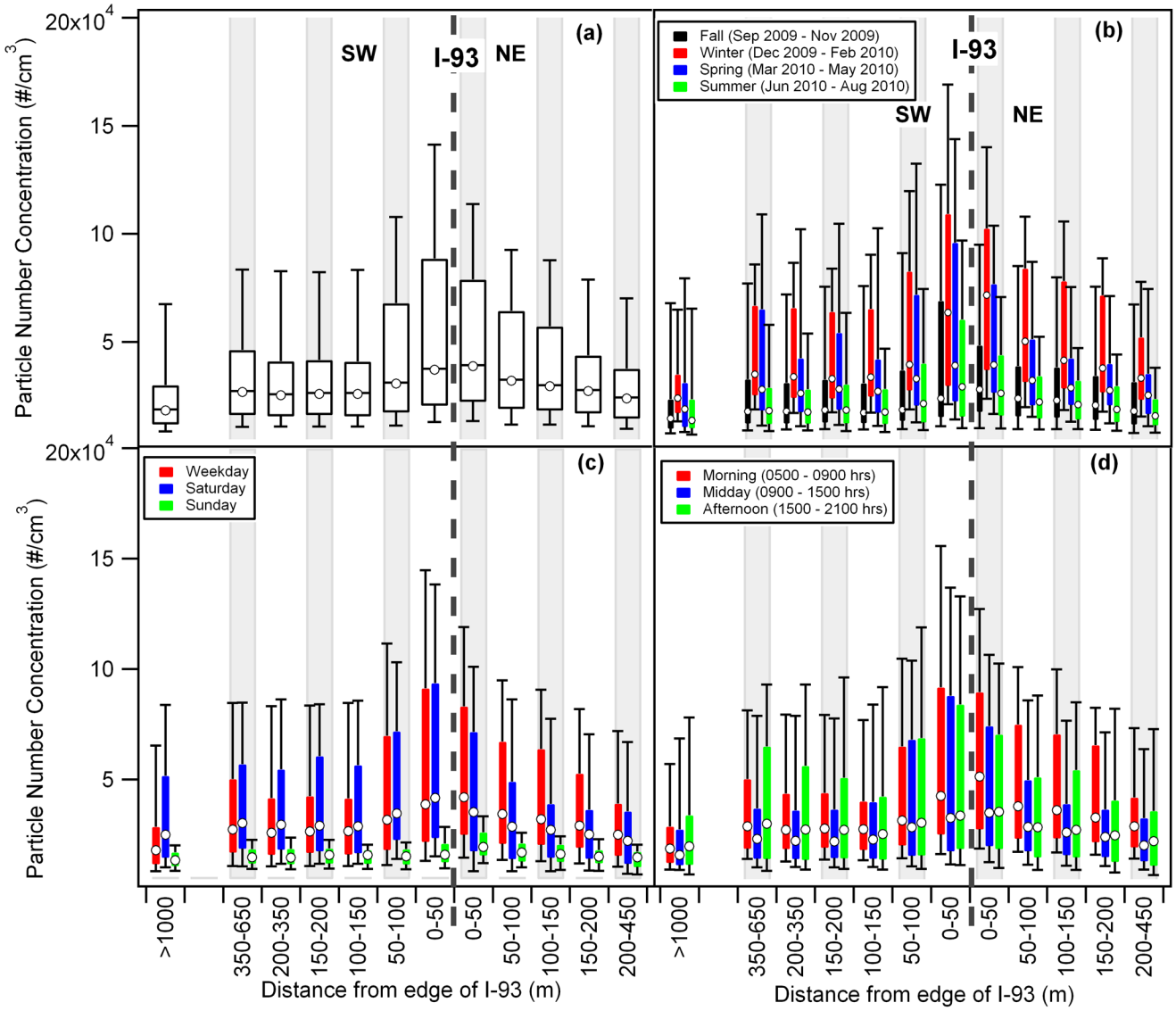

Figure 4.

Box plots of 1-second PNC measurements as a function of distance from I-93 for (a) all monitoring times as well as for the measurements stratified by (b) season, (c) day of the week and (d) time of day. The data in these plots represents 44 days of mobile monitoring. All distances are measured from the nearest edge of I-93.

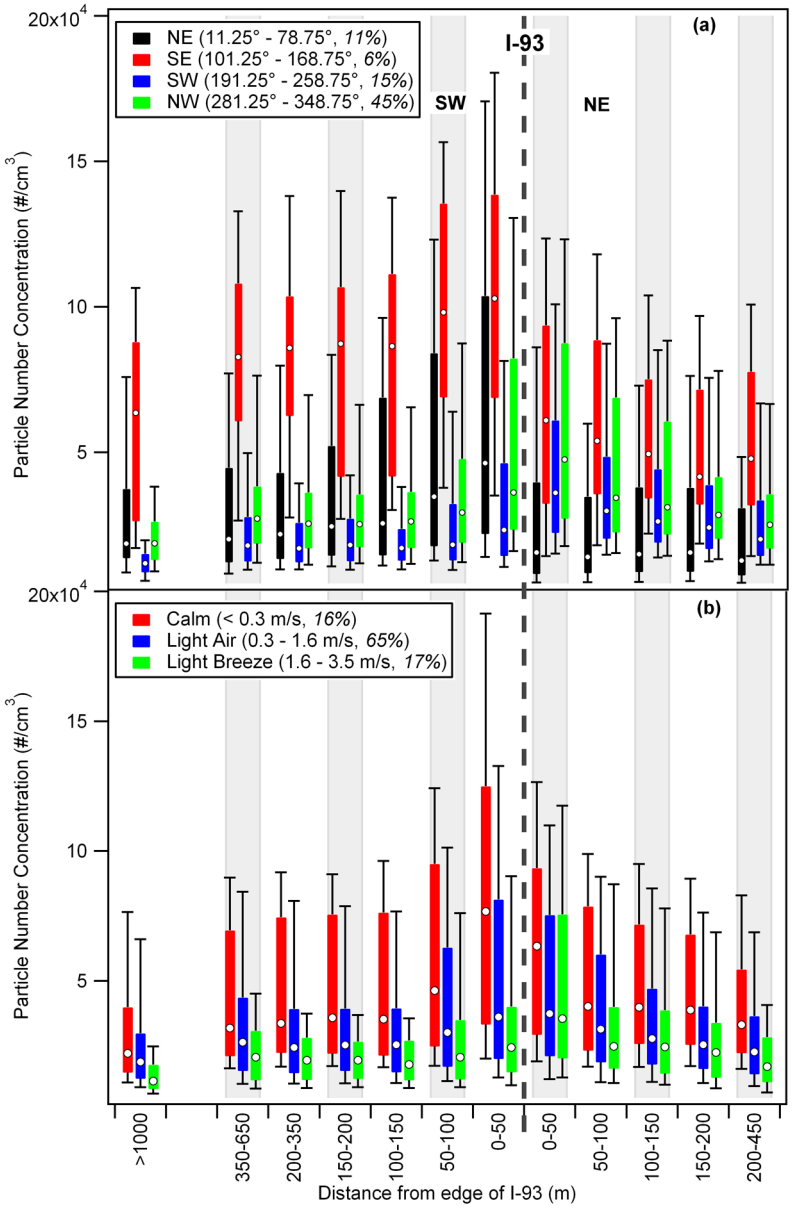

Figure 5.

Box plots of 1-second PNC measurements as a function of distance from I-93 stratified by (a) wind direction and (b) wind speed. The italicized numbers in the legend represent the fraction of monitoring hours that the wind was from the indicated direction. The data in these plots represents 44 days of mobile monitoring. All distances are measured from the nearest edge of I-93; wind speeds were calculated based on u_{35} using a powerlaw function (see section 2.2).

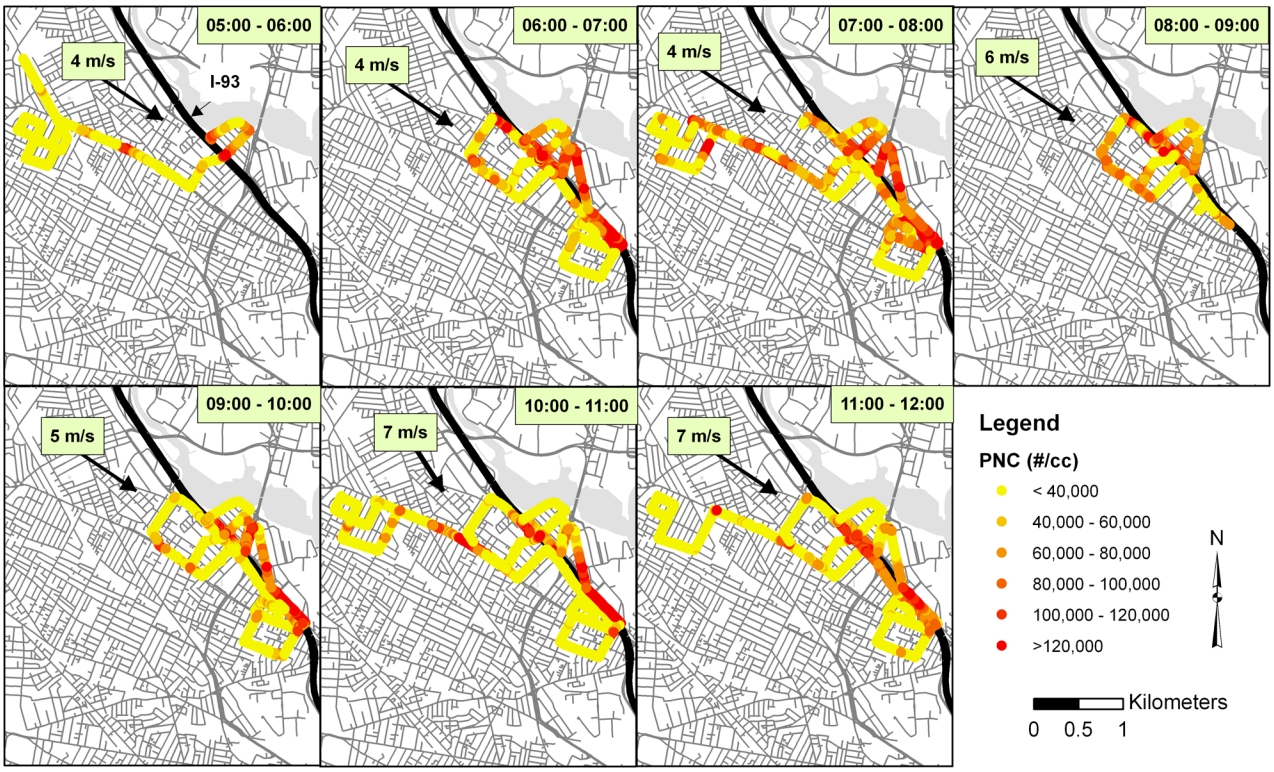

Figure 6.
PNC spatial distribution plots for the study area based on mobile monitoring measurements made on January 6, 2010. Each plot represents ~1 h of data collected at a frequency of 1 s^{-1}. The prevailing wind speed and direction are noted in the upper left corner of each plot.

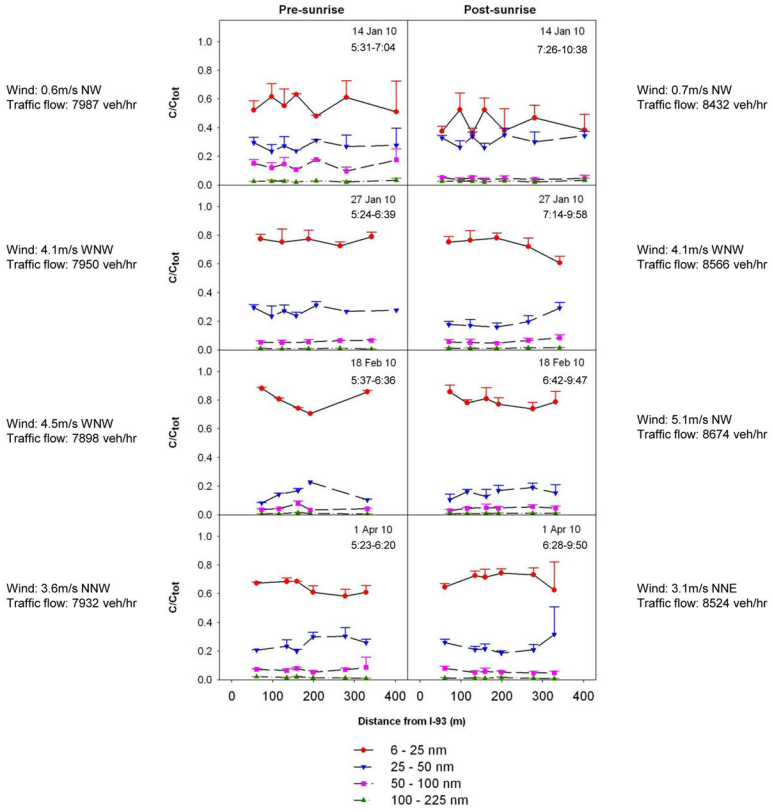

Figure 7.
Pre- and post-sunrise particle size distribution measurements for four days in 2010.

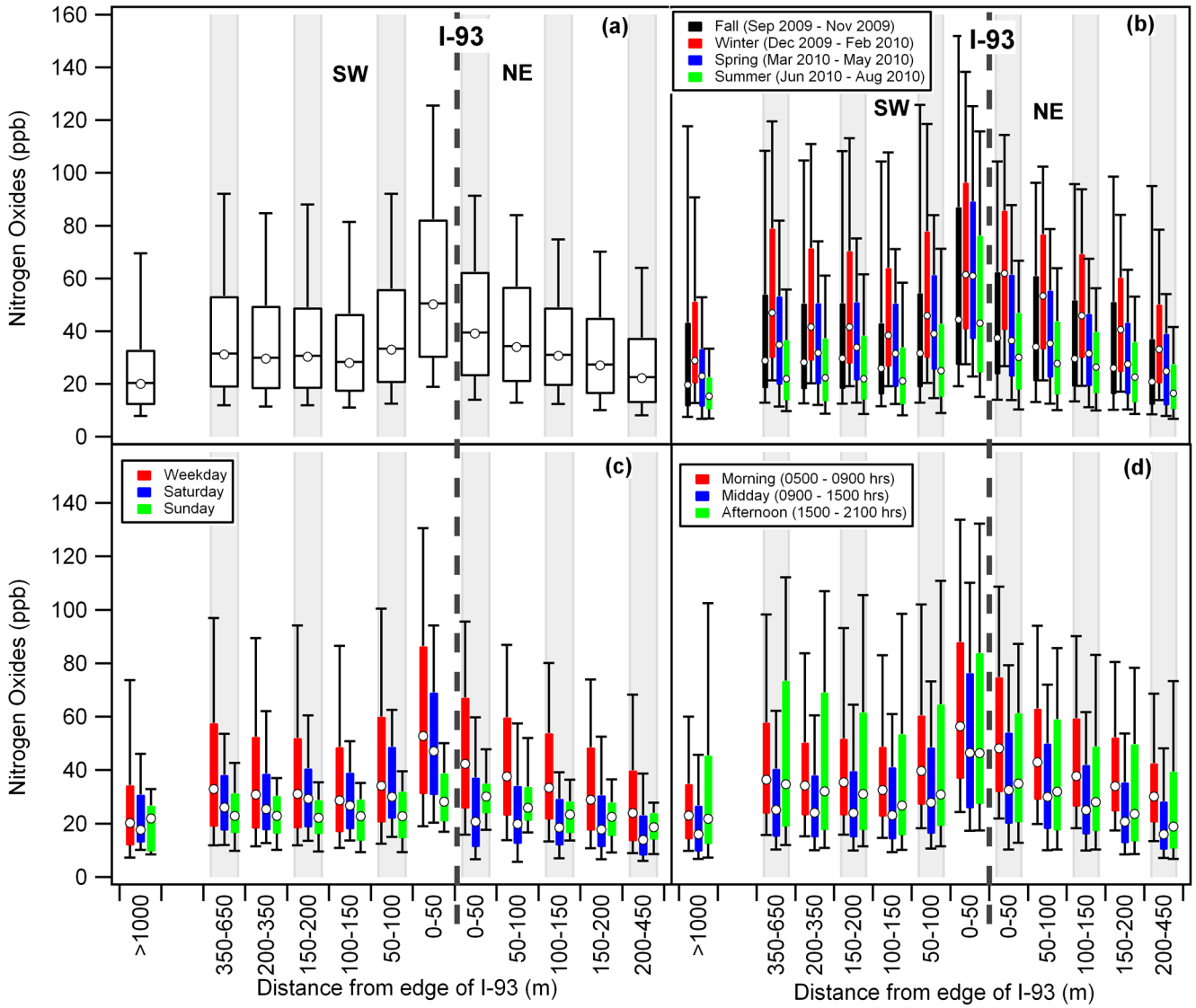

Figure 8.

Box plots of 20-s NO_x measurements as a function of distance from I-93 for (a) all monitoring times as well as for the measurements stratified by (b) season, (c) day of the week and (d) time of day. The data in these plots represents 44 days of mobile monitoring. All distances are measured from the nearest edge of I-93.

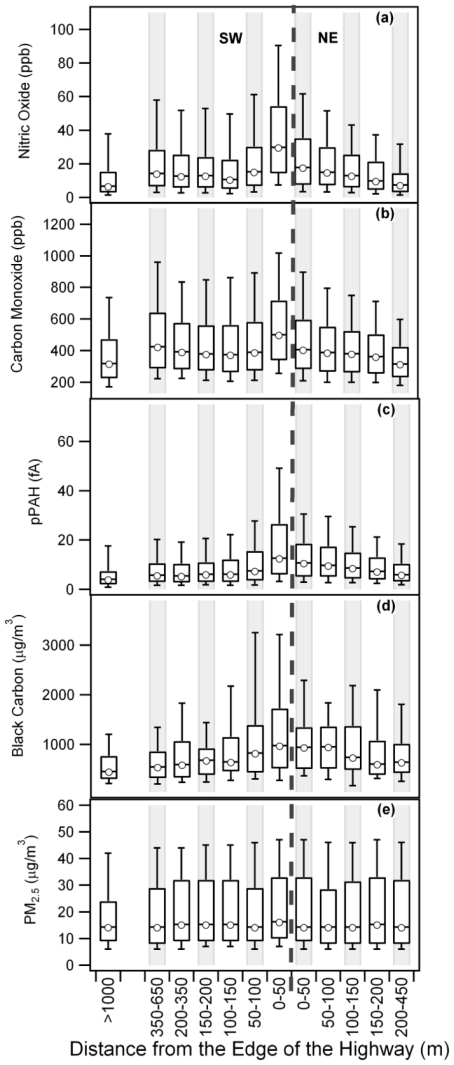

Figure 9.

Box plots of (a) NO, (b) CO, (c) pPAH, (d) BC and (e) $PM_{2.5}$ measurements as a function of distance from I-93 for all monitoring times. The data in these plots represents 37 days of mobile monitoring for NO, 39 days for CO, 38 days for pPAH, 10 days for BC, and 19 days for $PM_{2.5}$. All distances are measured from the nearest edge of I-93.

Table 1

Mobile monitoring times and dates (September 10, 2009 August 26, 2010).

Times	N	Weekdays[1]	Weekends[1]
Morning 04:30–10:30	35	Fall: Sep 10, Sep 18, Oct 6, Oct 20, Nov 17	Fall: Sep 20, Nov 8
		Winter: Dec 1, Dec 14, Jan 6, Jan 12, Jan 14, Jan 27, Feb 1, Feb 10, Feb 18	Winter: Dec 19, Feb 13
		Spring: Mar 2, Mar 9, Apr 1, Apr 7, Apr 15, May 4, May 6, May 11, May 13	Spring: May 22
		Summer: Jun 9, Jun 30, Jul 14, Jul 21, Aug 3, Aug 13	Summer: July 31
Midday 10:30–14:00	8	Fall: Sep 22, Oct 8, Nov 19	Winter: Feb 20, Feb 21
		Spring: Mar 6	
		Summer: Jun 16, Jun 24	
Afternoon 14:00–20:00	15	Winter: Dec 17, Jan 7, Jan 19, Jan 21, Feb 3	Fall: Oct 4, Oct 17
		Spring: Mar 10, Apr 12	
		Summer: Jun 2, Jul 29, Aug 26	

[1]The seasons were defined as follows (average seasonal temperature and relative humidity (RH) are provided parenthetically): Fall = September 10, 2009 – November 2009 (12 °C and 74% RH); Winter = December 2009 – February 2010 (−1 °C and 68% RH); Spring = March 2010 – May 2010 (13 °C and 61% RH); Summer = June 2010 – August 26, 2010 (23 °C and 70% RH).

Table 2

Air pollution monitoring equipment in the Tufts Air Pollution Monitoring Laboratory.

Parameter	Equipment; manufacturer/model	Detection limit	Instrument reporting interval (sec)	Averaging time (sec)	Lag time (sec)[1]
Particle number concentration (PNC)	Condensation Particle Counter (CPC) TSI (3775)	<1 particle/cm^3	1	1	3
Particle Size Distribution	Scanning Mobility Particle Sizer (SMPS); TSI Classifier (3080) TSI Nano DMA (3085)	<1 particle/cm^3	120	120	3
NO/NO$_x$	Chemiluminescence analyzer; Thermo Scientific 42i	0.40 ppb	1	20	30
CO	Gas filter correlation analyzer; Thermo Scientific 48i-TLE	0.04 ppm	1	10	30
Particle-bound polycyclic aromatic hydrocarbon (pPAH)	Photoelectric aerosol sensor; Ecochem Analytics PAS2000	6 femtoamps	8	8	10
Black carbon (BC)	Aethalometer; Magee Scientific AE-16	0.1 μg/m^3	60	60	N/A[2]
PM$_{2.5}$	Laser Photometer; TSI SIDEPACK AM510	0.001 mg/m^3	10	10	0
Latitude/ longitude	GPS receiver; Garmin GPS V	NA	1	1	0

[1] Lagtimes, the sum of the tubing residence time and instrument response time, were determined experimentally.

[2] NA = not applicable. The time lag was negligible compared to the averaging time.

Table 3

Spearman correlation ρ^2 for 120-s-averaged pollutant concentrations measured on June 9, 2010.

	CO	NO	NO_2	NO_x	PAH	$PM_{2.5}$	BC
PNC	**0.54**	**0.78**	**0.59**	**0.82**	**0.71**	**0.45**	**0.39**
CO		**0.77**	**0.51**	**0.77**	**0.51**	0.01	0.16
NO			**0.62**	**0.95**	**0.75**	**0.39**	**0.41**
NO_2				**0.79**	**0.60**	**0.21**	0.10
NO_x					**0.77**	**0.36**	**0.34**
PAH						**0.50**	**0.35**
$PM_{2.5}$							**0.31**

All of the ρ^2 values that are bolded are statistically significant ($p<0.05$).